European Journal of Neuroscience, Vol. 8, pp. 1363–1376, 1996

Glutamate-enriched Inputs from the Mesopontine Tegmentum to the Entopeduncular Nucleus in the Rat

N. P. Clarke, J. P. Bolam and M. D. Bevan
MRC Anatomical Neuropharmacology Unit and Department of Pharmacology, Mansfield Road, Oxford OX1 3TH, UK

Keywords: basal ganglia, glutamate, midbrain extrapyramidal area, pedunculopontine nucleus

Abstract

In order to clarify the origin and to examine the synaptology of the projection from the mesopontine tegmentum to the entopeduncular nucleus, rats received discrete deposits of anterograde tracers in different regions of the mesopontine tegmentum. Anterogradely labelled fibres in the entopeduncular nucleus were analysed at the light and electron microscopic levels. To determine the neurochemistry of the projection, the distributions of GABA and glutamate immunoreactivity in anterogradely labelled boutons in the entopeduncular nucleus were studied by postembedding immunocytochemistry. The morphological characteristics of anterogradely labelled structures were compared to those of choline acetyltransferase-immunopositive structures. The anterograde tracing demonstrated that the projection to the entopeduncular nucleus arises from the area defined by the cholinergic neurons of the pedunculopontine region and from the more medial and largely non-cholinergic, midbrain extrapyramidal area. The anterogradely labelled terminals formed asymmetrical synaptic contacts with dendritic shafts, cell bodies and more rarely spines in the entopeduncular nucleus, and they were significantly enriched in glutamate immunoreactivity compared to identified GABAergic terminals in the same region. The morphology, trajectory and synaptology of the anterogradely labelled fibres showed similarities to those of choline acetyltransferase-immunopositive fibres and terminals, providing indirect evidence in support of previous suggestions that at least part of the projection is cholinergic. The structures postsynaptic to the anterogradely labelled boutons also received input from other classes of terminals that had the morphological and neurochemical characteristics of boutons derived from the neostriatum, globus pallidus and subthalamic nucleus. These findings imply that the mesopontine tegmentum sends a projection to the entopeduncular nucleus that is heterogeneous with respect to its origin and also possibly its neurochemistry. The synaptology of the projection underlies one route through which the mesopontine tegmentum can exert effects on movement by modulating the direct and indirect pathways of information flow through the basal ganglia.

Introduction

The entopeduncular nucleus (EP) and its equivalent in primates, the internal segment of the globus pallidus, together with the substantia nigra pars reticulata represents the major output nuclei of the basal ganglia. As such, the activity of neurons in these nuclei conveys integrated basal ganglia information to the thalamus and/or subcortical premotor neurons. In view of the importance of these neurons in the expression of basal ganglia function it is necessary to understand the origin and nature of their afferent synaptic input, i.e. inputs that ultimately control the output of the basal ganglia. To this end the afferents of the EP have been extensively studied at both light and electron microscopic levels, and it is clear that the descending inputs derived from the neostriatum, globus pallidus and subthalamic nucleus have a highly ordered and specific pattern of termination (Bolam and Smith, 1992; Bolam *et al.*, 1993; Bevan *et al.*, 1994).

One of the ascending inputs to the EP is derived from the mesopontine tegmentum (MTg), which is an interface for many neuronal circuits and has been reported to be involved in many functions including locomotion (for review see Garcia-Rill, 1991), arousal and sleep-wake mechanisms (for review see Jones, 1993). One of the ways the MTg may influence movement is by its widespread projections to various nuclei of the basal ganglia (Lavoie and Parent, 1994c; Bevan and Bolam, 1995; Futami *et al.*, 1995). Although the projection to the EP has been examined at the light microscopic level (Graybiel, 1977; DeVito *et al.*, 1980; Jackson and Crossman, 1983; Saper and Loewy, 1982; Woolf and Butcher, 1986; Rye *et al.*, 1987; Lee *et al.*, 1988; Spann and Grofova, 1989; Steininger *et al.*, 1992; Charara and Parent, 1994; Lavoie and Parent, 1994b) and by electrophysiological techniques (Gonya-Magee and Anderson, 1983; Scarnati *et al.*, 1988), little is known about its synaptology and neurochemistry.

The precise neuronal origin of the projection from the MTg to the EP, and to the basal ganglia in general, has been the subject of much debate. It has been variously proposed that the projection arises almost exclusively from either the cholinergic neurons of the pedunculopontine region (PPN-Ch5) or the midbrain extrapyramidal area (MEA) (Woolf and Butcher, 1986; Rye *et al.*, 1987; Lee *et al.*, 1988;

Correspondence to: Nick Clarke, MRC Anatomical Neuropharmacology Unit, Mansfield Road, Oxford OX1 3TH, UK

Received 19 December 1995, accepted 26 January 1996

Spann and Grofova, 1989). The first objective of the present study was therefore to gain an insight into the site(s) of origin of the projection from the MTg to the EP by placing discrete deposits of anterograde tracers in different parts of the MTg defined with respect to the location of cholinergic neurons, identified by nicotinamide adenine dinucleotide phosphate (NADPH)-diaphorase histochemistry (Vincent *et al.*, 1983).

There is an increasing body of evidence indicating that the MTg provides neurochemically heterogeneous inputs to the basal ganglia (Charara and Parent, 1994; Lavoie and Parent, 1994c; Bevan and Bolam, 1995; Futami *et al.*, 1995). Immunocytochemical studies using antibodies against glutamate or GABA have identified several neurochemically distinct populations of neurons in the MTg (Clements and Grant, 1990; Jones, 1990, 1993; Clements *et al.*, 1991; Lai *et al.*, 1993; Lavoie and Parent, 1994a, c). In view of the importance of GABA and glutamate in neurotransmission and the previous suggestions by Gonya-Magee and Anderson (1983) and Scarnati *et al.* (1988) that the MTg projection to the EP is excitatory in nature, the second objective of this study was to examine the amino acid content of the boutons and synaptic terminals in the EP that were derived from the MTg. This was achieved by combining anterograde tracing and quantitative postembedding immunocytochemistry for glutamate and/or GABA.

It has been suggested previously that there is a cholinergic component to the projection from the MTg to the EP (Wainer *et al.*, 1984; Woolf, 1991; Mesulam *et al.*, 1992). The third objective of the study was therefore to compare the morphology of the choline acetyltransferase (ChAT)-immunoreactive axons and the synaptic nature of their terminals with those of anterogradely labelled structures from the MTg.

Some of the findings of the present study have been published in abstract form (Clarke *et al.*, 1995).

Materials and methods

Preparation of tissue

All surgical procedures were carried out on male Sprague–Dawley rats (250–350 g; Charles River) whilst under deep anaesthesia, which was induced and maintained by intraperitoneal injection of pentobarbitone. Environmental conditions for the housing of the rats and all procedures carried out on them were in accordance with the Animals (Scientific Procedures) Act 1986. Injections of neuronal tracers were placed into specific regions of the MTg under stereotaxic guidance using coordinates derived from the atlas of Paxinos and Watson (1986).

To study the origin of the projection, sections from seven animals that had been used in a previous study (Bevan and Bolam, 1995) were examined in addition to another five animals injected to complete this study. *Phaseolus vulgaris* leucoagglutinin (n = 5) (PHA-L; 2.5% in 0.01 M phosphate buffer, pH 8.0; Vector Laboratories, Peterborough, UK) (Gerfen and Sawchenko, 1984) or biotinylated dextran amine (n = 7) (BDA; 10% in 0.9% sodium chloride; Molecular Probes, USA) (Veenman *et al.*, 1992) was delivered by iontophoresis into the MTg via glass micropipettes of 10–50 μm internal diameter, using a pulsed (7 s on, 7 s off) cathodal current (5–9 μA) over 10–30 min. Four to eight days later the animals were deeply anaesthetized and solutions were perfused via the ascending aorta using a peristaltic pump. Prior to perfusion with fixative, the blood was removed by rapid perfusion with 100 ml phosphate-buffered saline (0.01 M phosphate) (PBS) over 1–2 min. This was followed by perfusion with 300 ml of 1.5% glutaraldehyde and 2% paraformaldehyde in 0.1 M phosphate buffer, pH 7.4 (PB), over 20 min (n = 7), or by perfusion with 200 ml 0.1% glutaraldehyde and 3% paraformaldehyde in PB over 5 min followed by 200 ml of 3% paraformaldehyde in PB over 20 min (n = 5).

To study the neurochemistry of the projection three animals received pressure injections of 50 nl wheat germ agglutinin conjugated to horseradish peroxidase (WGA–HRP; 5% in 0.9% saline; Sigma) over 5 min using glass micropipettes of 40–70 μm internal diameter. They were perfused 24 h later with 300 ml of 2.5% glutaraldehyde and 2% paraformaldehyde in PB over 30 min, followed by 300 ml of PB over 15 min. Two unoperated animals, for ChAT immunocytochemistry, were perfused with 200 ml 0.1–0.5% glutaraldehyde and 3% paraformaldehyde in PB over 5 min followed by 100 ml of 3% paraformaldehyde in PB over 10 min.

Following fixation, the brains were removed from the cranium, divided into 5 mm thick coronal slices and stored in PBS at 4°C prior to further processing. Coronal sections (60 μm) of the injection sites and the entopeduncular nucleus were taken using a vibrating microtome and collected in PBS. Sections from animals used to study the origin of the projection and the unoperated animals were then treated with 1% sodium borohydride in distilled water for 5–20 min, washed many times in PBS and freeze-thawed as described previously (von Krosigk and Smith, 1991).

Visualization of neuronal tracers

The BDA was visualized by incubation of the sections in an avidin–biotin–peroxidase complex (ABC; 1:100 dilution; Vector Laboratories) in PBS containing 1% bovine serum albumin overnight at room temperature or for 48 h at 4°C. Peroxidase linked to BDA by the avidin–biotin bridge was revealed by placing the sections in Tris buffer (0.05 M, pH 7.4) containing 0.025% diaminobenzidine and 0.006% hydrogen peroxide for 10–15 min. The reaction was terminated by rinsing several times in Tris buffer.

The PHA-L was visualized by incubating the sections in rabbit anti-PHA-L antibody (1:500–1000 dilution; Dakopatts, Denmark) overnight at room temperature or 48 h at 4°C. After many washes in PBS, the sections were incubated in a solution of biotinylated goat anti-rabbit IgG (1:100–200; Vector Laboratories) at room temperature for 2 h followed by a 2 h incubation in ABC (1:100). Bound peroxidase was revealed using diaminobenzidine as above. The antisera were diluted in PBS containing 1% bovine serum albumin and 2% normal goat serum.

The WGA–HRP was visualized using a modification of the tetramethylbenzidine (TMB)/tungstate method described by Weinberg and Van Eyck (1991). The sections were equilibrated in PB (pH 6.0) and then preincubated for 10 min in 10 ml of reaction mixture containing 9.2 ml PB (pH 6.0), 0.46 ml 1% ammonium paratungstate, 115 μl of 0.2% TMB in ethanol, 92 μl of 0.4% ammonium chloride and 92 μl of 20% D-glucose. The reaction was initiated by the addition of 10 μl of glucose oxidase (in 0.1 M sodium acetate, pH 4; Sigma), shaken frequently during the 2–5 min incubation, and then stopped by rinsing the sections three times in PB (pH 6.0). The TMB/tungstate reaction product was stabilized by incubating the sections in 5 ml of stabilization mixture, containing 5 mg diaminobenzidine in PB, 0.8 ml 1% cobalt chloride solution and 167.5 μl hydrogen peroxide, for 20 min. The sections were then rinsed three times in PB.

Immunocytochemistry for choline acetyltransferase

Sections were incubated in monoclonal antibody to choline acetyltransferase which was raised in rat–mouse hybrid cells (1:200–250; Boehringer Mannheim, Germany) overnight at room temperature or

for 48 h at 4°C. After several washes in PBS the sections were incubated in a solution of biotinylated goat anti-rat IgG (1:200; Vector Laboratories) for 2 h at room temperature, followed by a 2 h incubation in ABC. Bound peroxidase was revealed using diaminobenzidine as described above. The immunoreagents were diluted in PBS containing 2% bovine serum albumin and 2% normal goat serum.

Histochemistry for NADPH-diaphorase

Following the visualization of the neuronal tracers, sections of the MTg from the BDA- and PHA-L-injected animals were processed for the visualization of NADPH-diaphorase-positive neurons. These sections were incubated in a solution containing 0.1% NADPH (Sigma), 0.1% nitroblue tetrazolium (Sigma) and 0.3% Triton X-100 dissolved in Tris–HCl (0.05 M, pH 7.4) at 37°C for 5–30 min (Vincent *et al.*, 1983). The reaction was terminated by rinsing the sections several times in Tris buffer (0.05 M, pH 7.4). These sections were then mounted on gelatin-coated slides and processed for standard light microscopy.

Processing of sections for electron microscopy

Sections from the EP of all animals were placed flat at the bottom of a Petri dish and postfixed in 1% osmium tetroxide (Oxchem, UK) (in 0.1 M PB at pH 7.4) for 30 min. They were then washed in PB and rapidly dehydrated through a graded series of dilutions of alcohol. To enhance the contrast of the tissue in the electron microscope, the sections were stained with 1% uranyl acetate (Taab, UK) at the 70% alcohol phase. The sections were placed in two washes of propylene oxide for 10 min and then in resin (Durcupan, Fluka) overnight. Finally, the sections were embedded in resin on microscope slides, placed in an oven and cured for 48 h at 60°C.

Analysis of material

The injection sites in the MTg and the distribution of NADPH-positive neurons were analysed in the light microscope, drawn and photographed. Sections of EP from animals that had received BDA or PHA-L and from the unoperated animals that had been immunolabelled for ChAT were also drawn and/or photographed. Selected areas of the EP that were rich in labelled structures were cut out from the slides and glued to blank resin blocks. Serial ultrathin sections were cut on a Reichert–Jung Ultracut-E ultramicrotome and collected on Pioloform-coated copper slot grids. The ultrathin sections were contrasted with lead citrate for 1–2 min and examined in a Philips 410 electron microscope.

To compare the morphology and the nature of the postsynaptic targets of terminals anterogradely labelled from the MTg and terminals immunopositive for ChAT, all parts of ultrathin sections were scanned at a constant magnification. All labelled terminals forming synaptic contacts were photographed and classified according to their origin, morphology and nature of the postsynaptic target. Cross-sectional areas of labelled terminals and their synaptic targets were determined from photographs using a digitizing pad and MacStereology software. The cross-sectional areas were compared statistically using the Mann-Whitney *U*-test and a level of $P < 0.05$ was considered significant.

Postembedding immunocytochemistry for GABA and glutamate

In order to test for the presence of fixed glutamate and GABA in anterogradely labelled and non-labelled terminals in the EP of the WGA–HRP-injected animals, ultrathin sections were collected in series as pairs or triplets on gold, Pioloform-coated grids and labelled by the postembedding immunogold method. Glutamate-like and GABA-like immunoreactivity (hereafter referred to as glutamate and GABA immunoreactivity respectively) were detected using polyclonal antisera directed against fixed amino acid–protein complexes.

Pairs or triplets of sections from a series were immunolabelled on alternate grids to reveal glutamate and GABA immunoreactivity using a slight modification of the method described by Phend and co-workers (1992). The grids were first washed in 0.05 M Tris buffer (pH 7.6) containing 0.9% NaCl and 0.01% Triton X-100 (TBS–Triton) and then incubated overnight at room temperature on drops of a 1:5000 dilution of rabbit anti-glutamate antiserum (Arnel Products, New York; Hepler *et al.*, 1988; Petrusz *et al.*, 1990; Abdullah *et al.*, 1992) or a 1:15 000 dilution of rabbit anti-GABA antiserum (code 9; Hodgson *et al.*, 1985; Somogyi and Hodgson, 1985; Somogyi *et al.*, 1985) in TBS–Triton. After several washes in TBS–Triton and one wash in TBS at pH 8.2, the grids were incubated for 1–1.5 h at room temperature in a 1:25 dilution of 15 nm gold-conjugated goat anti-rabbit IgG (BioCell, Cardiff, UK) in TBS at pH 8.2. The grids were washed in TBS at pH 8.2 and then in water, stained with 1% aqueous uranyl acetate for 1–1.5 h and then with lead citrate. The sections were then examined in the electron microscope.

Analysis and quantification of glutamate- and GABA-immunolabelled material

Immunoreactivity for glutamate or GABA was detected by the presence of the electron-dense immunogold particles overlying labelled and unlabelled structures. In order to quantify the immunoreactivity, the cross-sectional areas of terminals and blood vessels in micrographs were calculated with the aid of a digitizing pad and MacStereology software. These values were then used to calculate the density (particles/μm^2) of immunogold particles overlying anterogradely-labelled and non-anterogradely-labelled boutons or terminals. The values were then corrected for non-specific binding of the antibodies to tissue-free resin by subtracting the density of gold particles overlying the lumen of capillaries in the same ultrathin section. The corrected density of immunogold particles overlying terminals and boutons in glutamate-labelled sections was normalized and referred to as the index of glutamate immunoreactivity, by expressing it as a ratio of that overlying striatal-like terminals (average of seven terminals per section), i.e. terminals that have the morphology of striatal terminals, form symmetrical synapses and have previously been shown to be GABAergic (Bolam and Smith, 1992; Bolam *et al.*, 1993). In order to control for the variability in immunolabelling on different days, between grids on the same run, or even between sections on the same grid, the immunogold particle density overlying striatal-like terminals in the same section was used when the data were normalized.

The density of immunogold particles overlying terminals and boutons on GABA-labelled sections was also normalized (index of GABA immunoreactivity), but in this case by expressing it as the ratio of the density overlying boutons that have the morphology of terminals derived from the subthalamic nucleus, form asymmetrical synapses and have previously been shown to be glutamate-positive (average of six terminals per section) (Smith and Parent, 1988; Nakanishi *et al.*, 1991; Bolam *et al.*, 1993; Bevan *et al.*, 1994). Issues concerning the quantification of immunolabelling have been discussed extensively on a previous occasion (Bevan *et al.*, 1995).

Anterogradely labelled and non-anterogradely labelled boutons or synaptic terminals encountered during systematic scanning of the glutamate-immunolabelled ultrathin sections were photographed and the density of immunogold particles overlying them was calculated

and normalized as described above. Most of the anterogradely labelled structures and some of the non-anterogradely labelled structures were examined and photographed in the next or next-but-one section that was GABA-labelled. The glutamate and GABA immunoreactivities of populations of boutons were compared statistically using the Mann–Whitney *U*-test and a level of $P < 0.05$ was considered significant.

Results

Light microscopic analysis

Injection sites in the MTg

Seven BDA injections (Fig. 1A–C, G–J, C′, G′) and five PHA-L injections (Fig. 1D–F, K–L, K′) were made in the MTg. The injection sites were characterized by neurons densely filled, in Golgi-fashion, with brown diaminobenzidine reaction product. The diaminobenzidine used to visualize the tracers was easily distinguishable from NADPH-diaphorase-positive neurons (cholinergic neurons) that were identified by the blue-purple reaction product that labelled their proximal regions [see Fig. 1A, B of Bevan and Bolam (1995) for colour micrographs of injections illustrated in our Fig. 1B, F].

The injection sites could be roughly divided into three groups. (i) Injections largely confined to the PPN-Ch5 (Butcher and Semba, 1989) ($n = 5$) (Fig. 1A–E, C′). (ii) Injections involving both the PPN-Ch5 and the MEA ($n = 5$) (Fig. 1F–J, G′). (iii) Injections placed in the MEA and thus largely avoiding the PPN-Ch5 ($n = 2$) (Fig. 1K, L, K′).

The mesopontine tegmental projection to the entopeduncular nucleus

The injections localized discretely in the PPN-Ch5 (Fig. 1A–E, C′) and injections localized discretely in the MEA (Fig. 1K, L, K′) led to anterograde labelling in the ipsilateral EP (Fig. 2A, B) and to a lesser extent in the contralateral EP. Consistent with these observations, injections that included both the PPN-Ch5 and the MEA (Fig. 1F–J, G′) also resulted in anterograde labelling in the EP. As all the material in the present study was prepared for electron microscopy and the sizes of the tracer deposits varied, it was not possible to make quantitative estimates of the density of the projections. Nevertheless, the anterogradely labelled fibres resulting from each of the three groups of injections had a similar morphology; they ranged from thick fibres with multiple varicosities to thin fibres that had relatively few varicosities. The thick and thin fibres coursed in simple linear or branching fashion in mediolateral, rostrocaudal and dorsoventral directions. In 60 μm thick sections some fibres coursed over large areas of the EP whereas others were restricted to more discrete regions of the nucleus.

Cholinergic innervation of the entopeduncular nucleus

Cholinergic fibres were identified by immunocytochemistry for ChAT visualized by the brown diaminobenzidine reaction product (Fig. 2C–F). They were relatively rare and tended to be very thin and non-varicose (Fig. 2C–E), although occasional thicker varicose fibres (Fig. 2F) were observed. The ChAT-immunopositive fibres displayed a variety of trajectories. In addition to the axons and terminals, a few ChAT-immunopositive perikarya and dendrites were observed along the medial and lateral borders of the EP and were continuous with the cholinergic (Ch4) cells of the nucleus basalis of Meynert. These dendrites, like the terminal fibres, are very thin and slightly varicose and so could only be distinguished at the electron microscopic level.

Electron microscopic analysis

Anterogradely labelled structures

The electron microscopic analysis of anterogradely labelled structures was carried out on tissue from two animals, which were perfused with fixative containing 1.5% glutaraldehyde, one that had received an injection of BDA in the medial PPN-Ch5 (Fig. 1B) and one that had received an injection of BDA that included both the PPN-Ch5 and the MEA (Fig. 1H). Labelled structures were identified by the presence of the electron-dense diaminobenzidine reaction product that adhered to the outer surfaces of organelles, such as mitochondria, and the inner surface of plasma membranes. Reaction product was found in nerve terminals, dendrites and myelinated and unmyelinated axons. Terminals anterogradely labelled with BDA from the MTg (Fig. 3A–C) and those labelled with WGA–HRP (identified by the crystals of TMB reaction product; Figs 5 and 6) were of small to large size, were densely packed with round or pleomorphic synaptic vesicles and made asymmetrical synaptic contacts with dendritic shafts and cell bodies or occasionally spines. The asymmetrical synaptic specializations were occasionally associated with subsynaptic dense bodies (Fig. 3A, B). There were no significant differences between the sizes of the terminals labelled by either method, or between their postsynaptic targets (Fig. 4; Table 1).

Choline acetyltransferase-immunoreactive structures

The electron microscopic analysis of ChAT-immunopositive structures was carried out on the two unoperated animals. The ChAT-immunoreactive terminals (Fig. 3D, E) were of small to medium size, contained variable densities of round or pleomorphic synaptic vesicles and made asymmetrical synaptic contacts with dendritic shafts or spines.

The size of the anterogradely labelled terminals (Table 1) was significantly greater than the ChAT-immunopositive terminals (Mann–Whitney *U*-test, $P \leq 0.0001$), although the distribution of the cross-sectional areas of the ChAT terminals was included within the distribution of the cross-sectional areas of the anterogradely labelled terminals (Fig. 4). The sizes of the structures postsynaptic to the ChAT-immunopositive terminals were significantly ($P < 0.05$) smaller than those postsynaptic to the WGA–HRP-labelled terminals (Table 1).

Glutamate and GABA immunoreactivity in the entopeduncular nucleus

Postembedding immunocytochemistry for glutamate and GABA was carried out on sections from two animals that had received WGA–HRP injections. The pattern of glutamate and GABA immunolabelling in the EP was similar for both animals. Boutons forming asymmetrical synaptic contacts in the EP have levels of glutamate associated with them that are consistently higher than that associated with boutons forming symmetrical synaptic contacts. Boutons forming symmetrical synaptic contacts, on the other hand, exhibit levels of GABA immunoreactivity greater than that associated with any other structure including neurons, cell bodies and dendritic structures and the majority of terminals forming asymmetrical synaptic contacts.

The immunoreactivity associated with several populations of terminals and boutons, defined on the basis of their origin or morphology, was analysed quantitatively (Figs 5–8). Striatal-like terminals were defined as irregularly shaped terminals containing numerous round and ovoid synaptic vesicles, few mitochondria and forming symmetrical synaptic contacts. Pallidal-like terminals were defined as larger terminals that contained vesicles that did not fill the whole of the bouton but were congregated close to the active zone. The terminals

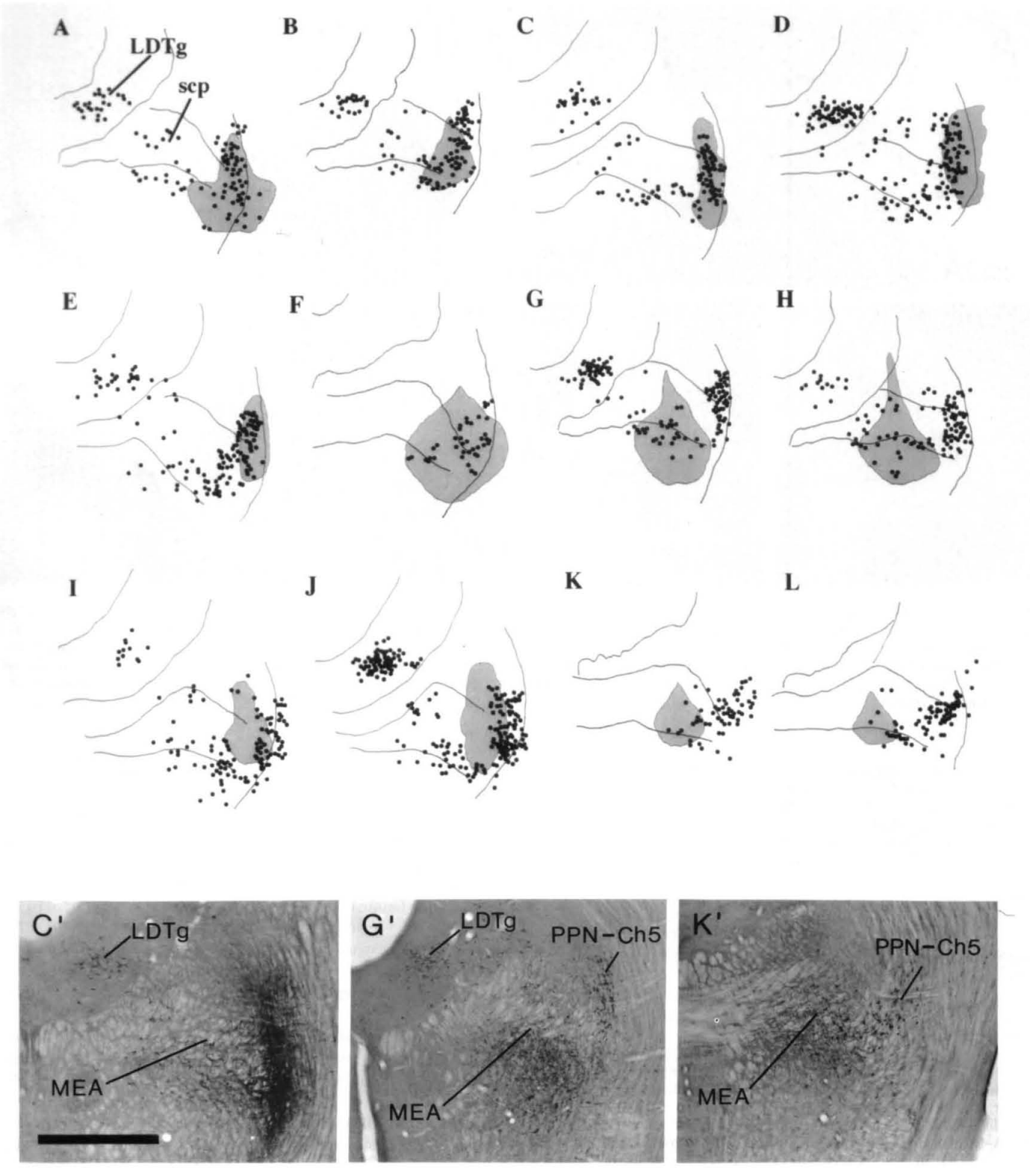

FIG. 1. (A–L) Schematic diagrams demonstrating the sites of twelve tracer deposits (shaded area) in the MTg (BDA, A–C, G–J; PHA-L, D–F, K, L) in relation to NADPH-diaphorase-positive (cholinergic) neurons, denoted by filled circles. The injection sites can be divided into three groups: (i) injections largely confined to the PPN-Ch5 (A–E); (ii) injections involving both the PPN-Ch5 and the MEA (F–J); (iii) injections placed in the MEA and largely avoiding the PPN-Ch5 (K, L). The micrographs C′, G′ and K′ are of the injection sites represented in the schematics C, G and K respectively. LDTg, laterodorsal tegmental region; MEA, midbrain extrapyramidal area; PPN-Ch5, region of the cholinergic neurons of the pedunculopontine nucleus; scp, superior cerebellar peduncle. All micrographs are at the same magnification; bar in C′ = 1 mm.

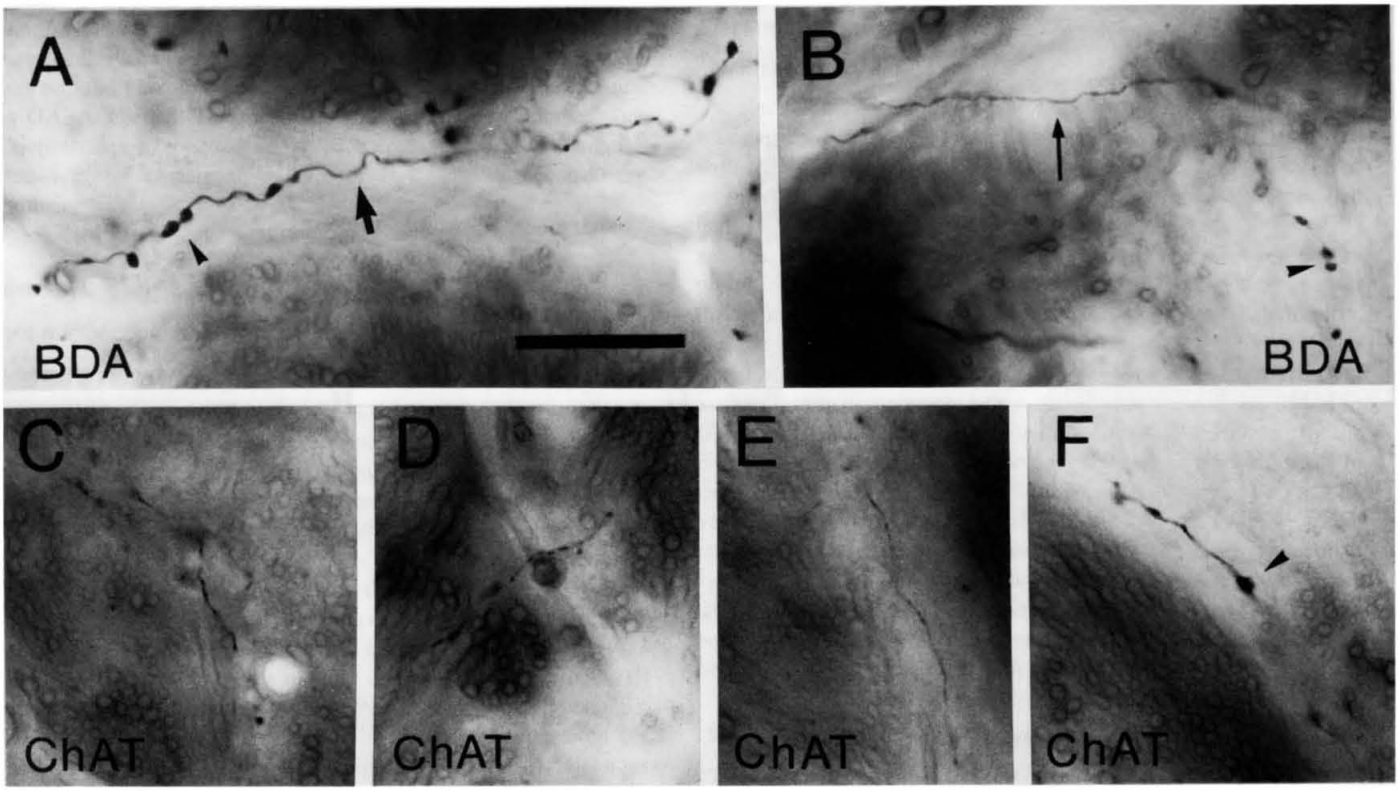

FIG. 2. (A–F) Light micrographs of anterogradely labelled fibres and ChAT-immunopositive fibres in the entopeduncular nucleus. The fibres anterogradely labelled from injections in the MTg (A–B) have either large (thick arrow) or small (thin arrow) diameter and display a range of trajectories. Varicosities (arrowheads) were more frequently observed on the thicker fibres. The anterograde fibres arose from an injection involving the PPN-Ch5 and the MEA (Fig. 1J). The fibres that are immunopositive for ChAT are generally thin and non-varicose (C–E), although there is an occasional thicker, varicose (arrowhead) fibre (F). These ChAT-immunopositive fibres are relatively rare in the entopeduncular nucleus and are also diverse in trajectory. All micrographs are at the same magnification; bar in A = 20 μm.

TABLE 1. Mean ± SEM, number and range of cross-sectional areas of ChAT-immunopositive terminals and terminals anterogradely labelled from the MTg with BDA or WGA–HRP, and the cross-sectional area of their postsynaptic targets in the entopeduncular nucleus.

	Terminal area	Postsynaptic target area
ChAT-immunopositive terminals	0.416 ± 0.04 μm² *n* = 23 range, 0.135–0.827 μm²	0.929 ± 0.211 μm² *n* = 23 range, 0.038–3.924 μm²
BDA-anterogradely labelled terminals	0.704 ± 0.05 μm² *n* = 32 range, 0.268–1.291 μm²	1.414 ± 0.273 μm² *n* = 31 range, 0.082–5.641 μm²
WGA–HRP-anterogradely labelled terminals	0.82 ± 0.09 μm² *n* = 32 range, 0.239–2.439 μm²	1.587 ± 0.238 μm² *n* = 28 range, 0.067–4.776 μm²

The anterogradely labelled terminals are significantly (Mann–Whitney *U*-test) larger than the ChAT-immunopositive terminals ($P \leq 0.0001$). The ChAT-immunopositive postsynaptic target areas are significantly smaller than the WGA–HRP-anterogradely labelled target areas ($P < 0.05$). The data on the cross-sectional areas of the terminals are illustrated graphically in Figure 4. *n*, number of terminals.

contained several mitochondria and formed symmetrical synaptic contacts. Subthalamic-like terminals were defined as medium-sized terminals containing small, round synaptic vesicles which congregated at the active zone, and forming asymmetrical synaptic contacts.

Striatal-like terminals. Terminals that displayed the morphological features typical of terminals derived from the neostriatum contained relatively low levels of glutamate immunoreactivity (mean ± SEM of index of glutamate immunoreactivity, 1.004 ± 0.043, $n = 82$) but high levels of GABA immunoreactivity (mean ± SEM of index of GABA immunoreactivity, 4.588 ± 0.191, $n = 120$). The levels of glutamate immunoreactivity were significantly (Mann–Whitney *U*-test) lower than those associated with terminals that displayed morphological features of subthalamic terminals ($P < 0.0001$), pallidal terminals ($P < 0.01$) or terminals anterogradely labelled from the MTg ($P < 0.0001$). The levels of GABA immunoreactivity were significantly greater than those associated with the three other terminal types ($P < 0.0001$ for subthalamic-like and anterogradely labelled boutons; $P < 0.05$ for pallidal-like).

Pallidal-like terminals. Terminals that displayed the morphological features typical of terminals derived from the globus pallidus had relatively low levels of glutamate immunoreactivity (mean ± SEM, 1.426 ± 0.156, $n = 13$) but high levels of GABA immunoreactivity (mean ± SEM, 3.432 ± 0.384, $n = 14$) associated with them. The levels of glutamate immunoreactivity were significantly lower than those associated with terminals that displayed morphological features of subthalamic terminals or terminals anterogradely labelled from the MTg ($P < 0.001$ in each case). The levels of GABA immunoreactivity were significantly greater than those associated with subthalamic-like terminals or terminals anterogradely labelled from the MTg ($P < 0.0001$ in each case).

Subthalamic-like terminals. Terminals that displayed the morphological features typical of terminals derived from the subthalamic nucleus had high levels of glutamate immunoreactivity (mean ± SEM, 2.439 ± 0.08, $n = 81$) but low levels of GABA immunoreactivity (mean ±

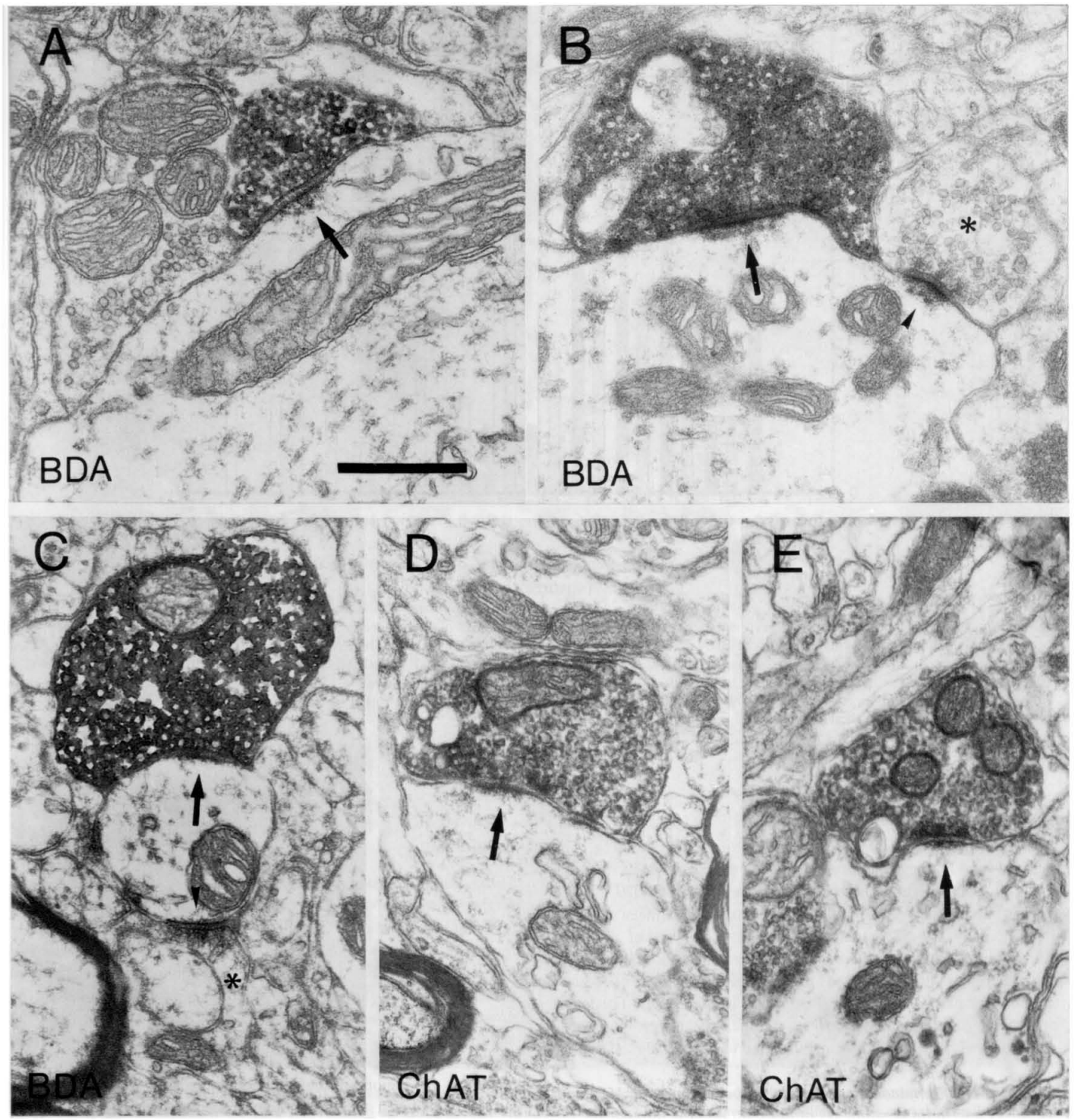

FIG. 3. (A–E) Electron micrographs illustrating the morphology of synaptic terminals anterogradely labelled from the MTg and those immunocytochemically labelled for ChAT in the entopeduncular nucleus. The synaptic terminals are filled with electron-dense peroxidase reaction product that was revealed using diaminobenzidine as the chromogen. Both the anterogradely labelled terminals (A–C) and the ChAT-immunopositive terminals (D, E) form asymmetrical synaptic contacts (arrows) with dendritic shafts of entopeduncular neurons. The terminals in A and C are anterogradely labelled from an injection largely confined to the PPN-Ch5 (Fig. 1B) and the terminal in B originates from an injection involving both the PPN-Ch5 and the MEA (Fig. 1H). In B the dendrite is receiving convergent synaptic input from the anterogradely labelled terminal and a non-anterogradely labelled terminal (asterisk) forming an asymmetrical synapse (arrowhead). In C the dendrite is receiving convergent synaptic input from the anterogradely labelled terminal and a non-anterogradely labelled terminal (asterisk) that is in symmetrical synaptic contact (arrowhead). All micrographs are at the same magnification; bar in A = 0.5 μm.

SEM, 0.999 ± 0.055, $n = 63$) associated with them. The levels of glutamate immunoreactivity were significantly greater than those associated with terminals that displayed morphological features of striatal terminals or pallidal terminals ($P < 0.0001$ in each case). The levels of GABA immunoreactivity were significantly lower than those associated with striatal-like or pallidal-like terminals ($P < 0.0001$).

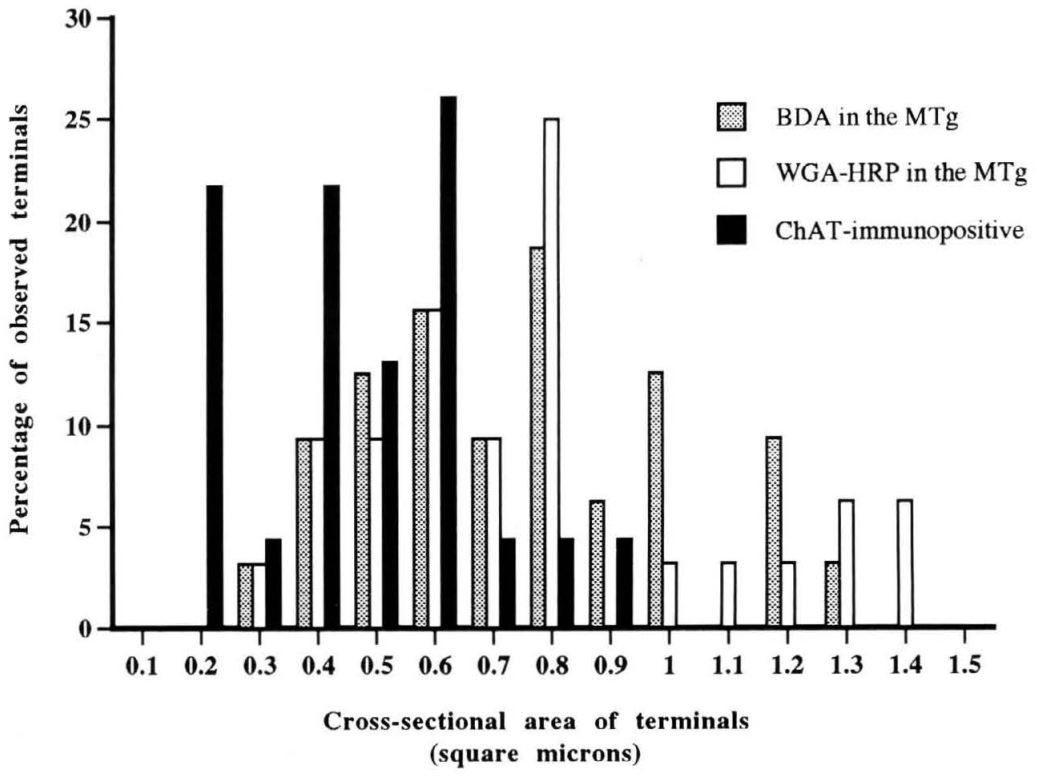

FIG. 4. Frequency distribution of the cross-sectional areas of synaptic terminals and boutons in the entopeduncular nucleus that were either ChAT-immunopositive or anterogradely labelled following injections of BDA or WGA–HRP in the mesopontine tegmentum. The terminals anterogradely labelled with BDA or WGA–HRP are significantly (Mann–Whitney *U*-test) larger than the ChAT-immunopositive terminals ($P < 0.0001$), although their distributions overlap. Two WGA–HRP-labelled terminals with cross-sectional areas of 2.146 and 2.439 μm^2 are omitted from the distribution for the sake of clarity. The mean ± SEM, number (n) and range of cross-sectional areas of ChAT-immunopositive, BDA-anterogradely labelled and WGA–HRP-anterogradely labelled terminals and their respective postsynaptic target areas are shown in Table 1.

Terminals and boutons anterogradely labelled from the MTg. The terminals and boutons anterogradely labelled from the MTg had high levels of glutamate immunoreactivity (mean ± SEM, 2.079 ± 0.09, $n = 54$) but low levels of GABA immunoreactivity (mean ± SEM, 1.1168 ± 0.09, $n = 52$) associated with them. The levels of glutamate immunoreactivity were significantly greater than those associated with terminals that displayed morphological features of striatal terminals or pallidal terminals ($P < 0.005$ in each case). The levels of GABA immunoreactivity were significantly lower than those associated with striatal-like or pallidal-like terminals ($P < 0.0001$).

Convergence of terminals anterogradely labelled from the MTg with the direct and indirect pathways of information flow through the basal ganglia on single entopeduncular neurons

Individual entopeduncular neurons were observed receiving convergent synaptic contact from terminals anterogradely labelled from the MTg and terminals that possessed the morphological and neurochemical characteristics of those derived from other basal ganglia nuclei. The anterogradely labelled terminals were observed making synaptic contact with dendrites that also received synaptic input from terminals that displayed the morphological and/or neurochemical characteristics of terminals derived from the neostriatum ($n = 26$), globus pallidus ($n = 2$) and subthalamic nucleus ($n = 3$) (Figs 3, 5 and 6). Convergent input from anterogradely labelled terminals and globus pallidus terminals also occurred on the perikarya of single EP neurons ($n = 3$).

Discussion

The major findings of this study provide new data concerning the origin, neurochemistry and synaptic organization of the mesopontine tegmental projection to the EP. The projection is predominantly ipsilateral and arises from both the PPN-Ch5 and the adjacent, largely non-cholinergic, MEA. The postembedding immunocytochemical data fulfil one of the criteria that glutamate is a neurotransmitter in the projection from the MTg to the EP by demonstrating that the anterogradely labelled terminals are glutamate-enriched compared to known GABAergic terminals. The fact that part of this projection arises in the region of the cholinergic neurons in the MTg, the similarity between the morphology, trajectory and synaptology of some of the anterogradely labelled fibres and ChAT-immunopositive fibres, and previous tracing studies suggest that one component of the projection might be cholinergic. These findings, together with the electron microscopic findings, support the hypothesis that the MTg sends glutamatergic and cholinergic projections to the EP, where at least one of the roles of the projection is to modulate the direct and indirect pathways of information flow through the basal ganglia.

The site of origin of the mesopontine tegmental projection to the entopeduncular nucleus

The use of small deposits of anterograde tracers combined with histochemical counterstaining for NADPH-diaphorase, which in

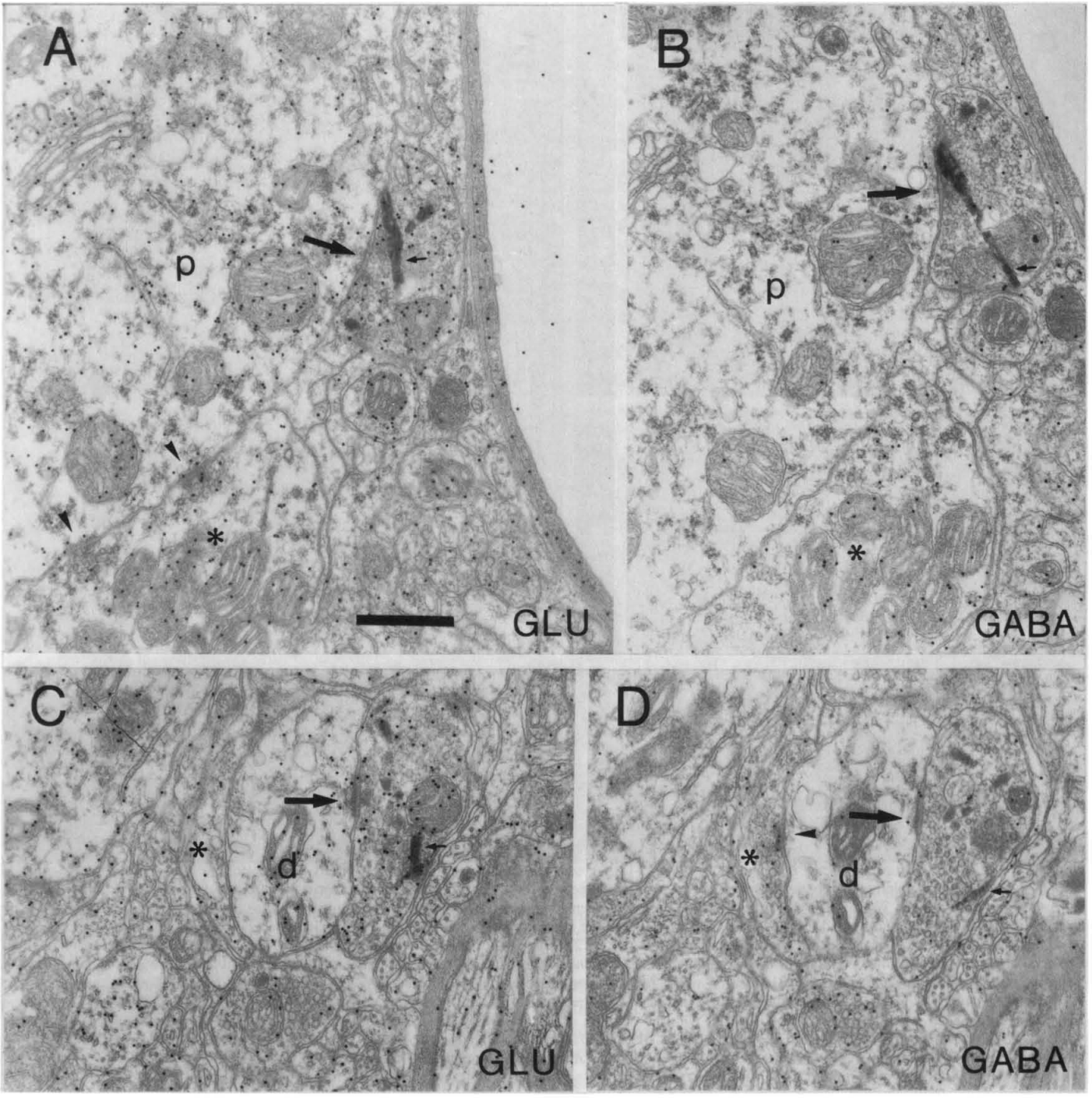

FIG. 5. Pairs of electron micrographs of serial sections of synaptic terminals in the entopeduncular nucleus that were anterogradely labelled from WGA–HRP injections in the MTg. The WGA–HRP was revealed using tetramethylbenzidine/tungstate which, unlike diaminobenzidine, forms crystals (small arrows). One of each pair has been immunolabelled for glutamate (A, C; GLU) and the other for GABA (B, D). The anterogradely labelled synaptic terminals are associated with relatively high indexes of glutamate immunoreactivity (A, 2.055; C, 2.977) and are GABA-immunonegative (B, 0.935; D, 1.155). They form asymmetrical synaptic contacts (arrows) with dendrites (d) or perikarya (p) of entopeduncular neurons. In A and B the anterogradely labelled terminal can be seen making synaptic contact with the perikaryon of a single entopeduncular neuron which receives symmetrical synaptic contact (arrowheads in A) from a pallidal-like terminal (asterisks). The index of glutamate immunoreactivity overlying the pallidal-like terminal is 1.708 and the index of GABA immunoreactivity is 2.772. In C and D the anterogradely labelled terminal makes synaptic contact with the dendrite of a single entopeduncular neuron which receives symmetrical synaptic contact (arrowhead in D) from a striatal-like terminal (asterisks). The striatal-like terminal is associated with a level of glutamate immunoreactivity of 1.001 and a level of GABA immunoreactivity of 6.767. All micrographs are at the same magnification; bar in A = 0.5 μm.

this region is a faithful marker of cholinergic neurons (Vincent *et al.*, 1983), enabled us to clarify the conflicting reports in the literature. We demonstrated that the area defined as the MEA (Rye *et al.*, 1987; Lee *et al.*, 1988), which consists largely of non-cholinergic neurons, provides a major innervation of the EP. We also demonstrate that the region we have defined as PPN-Ch5

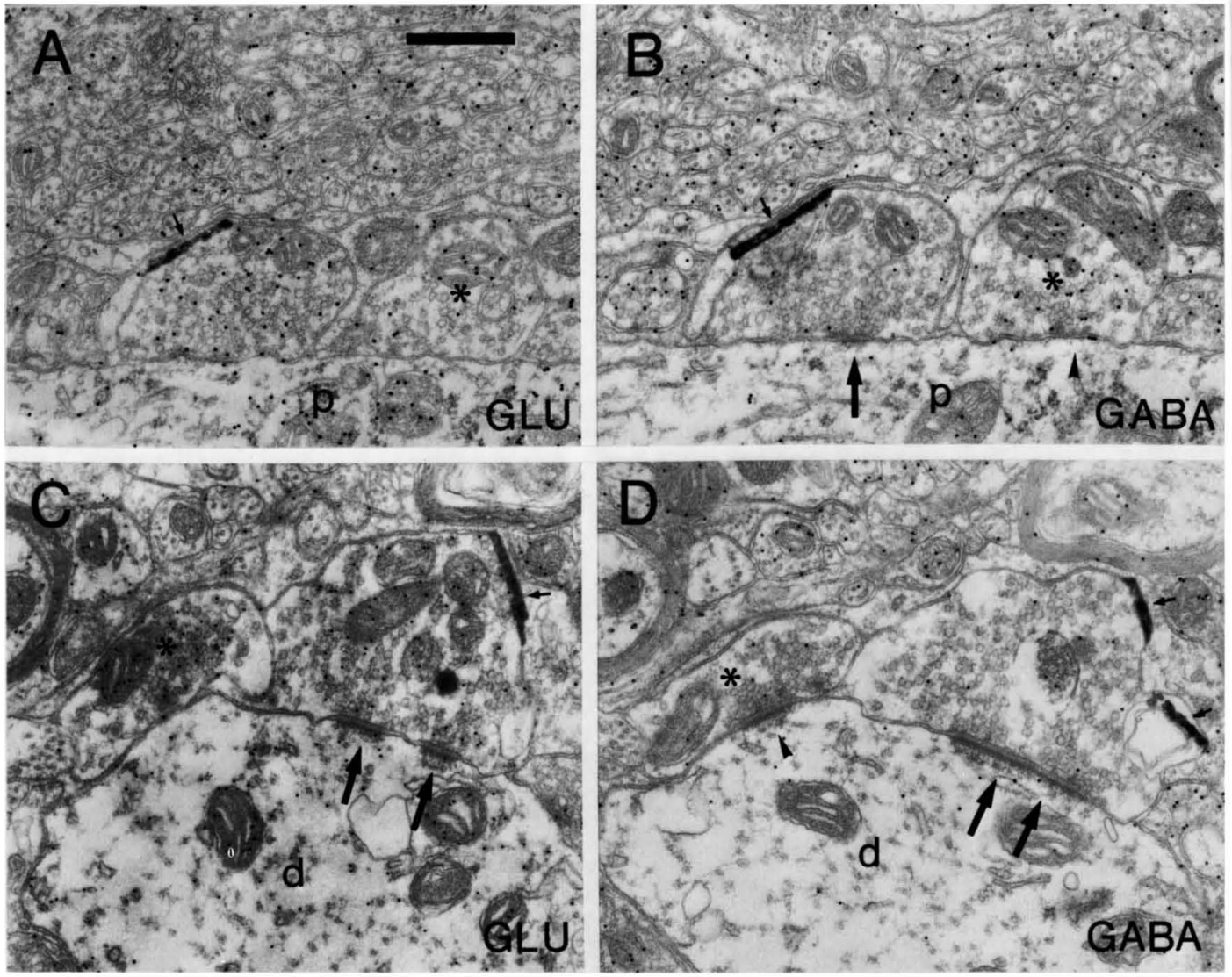

FIG. 6. Pairs of electron micrographs of serial sections of synaptic terminals in the entopeduncular nucleus that were anterogradely labelled from WGA–HRP injections in the MTg. The WGA–HRP was revealed using tetramethylbenzidine/tungstate which, unlike diaminobenzidine, forms crystals (small arrows). One of each pair has been immunolabelled for glutamate (A, C; GLU) and the other for GABA (B, D). The anterogradely labelled synaptic terminals are associated with relatively high indexes of glutamate immunoreactivity (A, 2.324; C, 2.129) and are GABA-immunonegative (B, 0.775; D, 0.387). They form asymmetrical synaptic contacts (arrows) with dendrites (d) or perikarya (p) of entopeduncular neurons. In A and B the anterogradely labelled terminal makes synaptic contact with the perikaryon of a single entopeduncular neuron which receives symmetrical synaptic contact (arrowhead in B) from a pallidal-like terminal (asterisks). The index of glutamate immunoreactivity overlying the pallidal-like terminal is 0.809 and the index of GABA immunoreactivity is 5.354. In C and D the anterogradely labelled terminal forms synaptic contact with the dendrite of a single entopeduncular neuron which receives an asymmetrical synaptic contact (arrowhead in D) from a subthalamic-like terminal (asterisks). The subthalamic-like terminal is associated with an index of glutamate immunoreactivity of 2.789 and an index of GABA immunoreactivity of 0.935. All micrographs are at the same magnification; bar in A = 0.5 μm.

(Bevan and Bolam, 1995), which includes the more laterally placed diaphorase-positive (i.e. cholinergic) neurons (Woolf and Butcher, 1986; Spann and Grofova, 1989) innervates the EP. It appears, therefore, that the mesopontine projection to the EP arises from both the cholinergic and non-cholinergic regions of the MTg and not exclusively from one region or the other (Woolf and Butcher, 1986; Lee *et al.*, 1988; Spann and Grofova, 1989).

Data derived from injections of tracers in the brainstem should be interpreted with caution due to the possibility of uptake by fibres of passage. However, there are no known projections to the EP or other regions of the basal ganglia from regions caudal to our deposits. Furthermore, each of our injections gave rise to a similar pattern of labelling in the EP and other regions of the basal ganglia (not illustrated).

Neurochemistry of the mesopontine tegmental projection to the EP

The postembedding immunocytochemistry for glutamate and GABA combined with the anterograde labelling revealed that anterogradely labelled terminals form asymmetrical synaptic specializations, are enriched in glutamate immunoreactivity and are GABA-immunonegative. Despite the ubiquitous distribution of glutamate in mammalian tissue, the levels that we detected in the anterogradely labelled terminals were significantly greater than in identified GABAergic terminals, i.e. terminals derived from the neostriatum or globus pallidus. The level of enrichment that we observed might be an underestimate of the true value as the density of immunogold particles was normalized with respect to GABAergic terminals that will, in

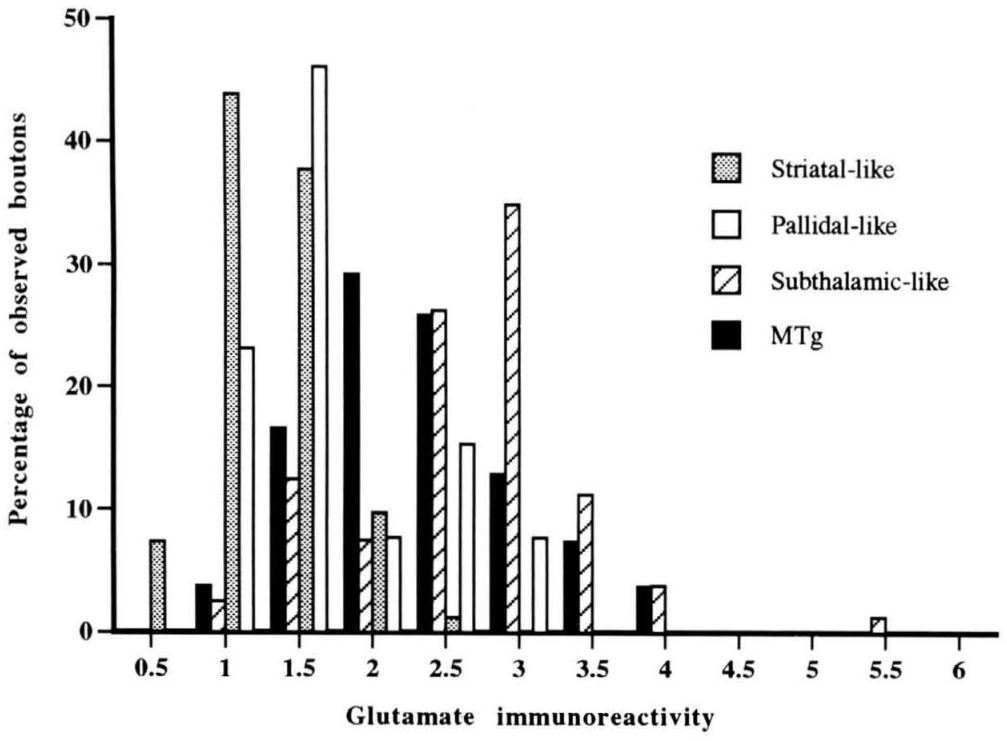

FIG. 7. Frequency distribution of the level of glutamate immunoreactivity associated with synaptic terminals and boutons in the entopeduncular nucleus that were either anterogradely labelled from the mesopontine tegmentum (MTg) or non-anterogradely labelled. The non-anterogradely labelled terminals were divided on morphological grounds into striatal-like, pallidal-like and subthalamic-like. Glutamate immunoreactivity is represented as the ratio of the density of immunogold particles overlying the synaptic terminal or bouton to that overlying striatal-like terminals forming symmetrical synapses in the same section. The anterogradely labelled and subthalamic-like terminals are significantly enriched in glutamate compared to the level found in striatal-like and pallidal-like synaptic terminals (Mann–Whitney *U*-test; $P < 0.005$).

addition to metabolic glutamate, contain glutamate required for the synthesis of GABA. It is also important to note that the index of glutamate immunoreactivity in the anterogradely labelled terminals was not significantly different from the index in subthalamic-like terminals, which are well established as being glutamatergic (Smith and Parent, 1988; Rinvik and Ottersen, 1993). Previous studies have demonstrated significant enrichment of glutamate immunoreactivity in known and putative glutamatergic terminals (Somogyi *et al.*, 1986; Ottersen, 1989; Ottersen and Storm-Mathisen, 1989; Van den Pol, 1991; Llewellyn-Smith *et al.*, 1992; Phend *et al.*, 1992; Rinvik and Ottersen, 1993; Kharazia and Weinberg, 1994; Valtschanoff *et al.*, 1994; Bevan *et al.*, 1995; Bevan and Bolam, 1995; Ericson *et al.*, 1995). Our finding of a significant enrichment of glutamate in the anterogradely labelled terminals fulfils one of the criteria that a substance is a neurotransmitter, implying therefore that the projection from the MTg to the EP is glutamatergic. This suggestion is consistent with the high levels of glutamate immunoreactivity found in neurons in the MTg of the rat (Clements and Grant, 1990; Clements *et al.*, 1991), cat (Lai *et al.*, 1993) and squirrel monkey (Lavoie and Parent, 1994a, c), and with the electrophysiological data on the projection (Gonya-Magee and Anderson, 1983; Scarnati *et al.*, 1988).

The similarity in the morphology and synaptology of the anterogradely labelled terminals and ChAT-immunopositive terminals, combined with the location of the tracer deposits in relation to identified cholinergic neurons in the PPN-Ch5 and previous combined retrograde labelling and immunocytochemical studies (Woolf and Butcher, 1986; Lee *et al.*, 1988), suggests that a component of the projection arises from the cholinergic neurons of the MTg. This is consistent with the presence of m3 muscarinic receptors in the EP (Levey *et al.*, 1994) and previous immunocytochemical studies (Woolf, 1991; Mesulam *et al.*, 1992). The fact that the overall distribution of the sizes of ChAT-positive terminals falls within the overall distribution of anterogradely labelled terminals, the difference in the mean sizes of the ChAT-immunopositive and the anterogradely labelled boutons (Table 1) and the location of the tracers deposits are in favour of both cholinergic and non-cholinergic components of the projection (Clements and Grant, 1990; Jones, 1990, 1993; Clements *et al.*, 1991; Spann and Grofova, 1992; Lavoie and Parent, 1994a, c). It should be noted that the larger cross-sectional area of the anterogradely labelled boutons is not a fixation artefact; it is in fact likely to be an underestimate, as the higher concentrations of glutaraldehyde used for the anterograde tracing would lead to more tissue shrinkage than the concentration used for ChAT immunocytochemistry (Hopwood, 1972). It must be remembered that our observations only provide indirect evidence of a cholinergic component of the projection from the MTg to the EP, and indeed it is also possible that the cholinergic terminals in the EP could arise from a previously unidentified cholinergic projection.

An important issue that remains to be addressed is the glutamate level in cholinergic terminals, as some of the cholinergic neurons in the pedunculopontine region have been shown to be strongly glutamate-immunoreactive (Clements and Grant, 1990; Clements *et al.*, 1991; Lavoie and Parent, 1994a, c). However the antibody against glutamate that we used was prepared against a glutamate–glutaraldehyde–protein conjugate (Hepler *et al.*, 1988; Petrusz *et al.*, 1990; Abdullah *et al.*, 1992); the relatively high levels of glutaraldehyde therefore required during fixation of the tissue were not compatible with immunocytochemistry for choline acetyltransferase. Thus for technical reasons

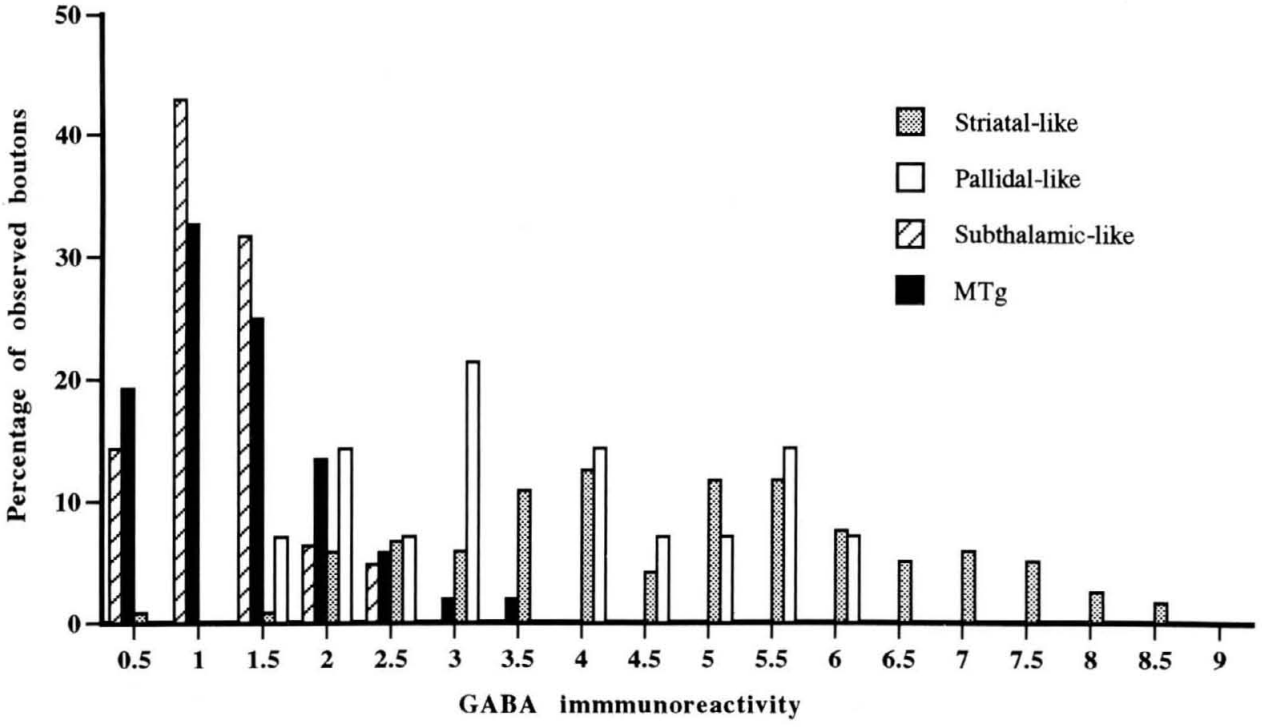

FIG. 8. Frequency distribution of the level of GABA immunoreactivity associated with synaptic terminals in the entopeduncular nucleus that were either anterogradely labelled from the mesopontine tegmentum (MTg) or non-anterogradely labelled. The non-anterogradely labelled terminals were divided on morphological grounds into striatal-like, pallidal-like and subthalamic-like. GABA immunoreactivity is represented as the ratio of the density of immunogold particles overlying the synaptic terminal or bouton to that overlying subthalamic-like terminals forming asymmetrical synapses in the same section. The striatal-like and pallidal-like terminals are significantly enriched in GABA compared to the levels found in anterogradely labelled and subthalamic-like synaptic terminals (Mann–Whitney U-test; $P < 0.0001$). Two striatal-like terminals with levels of GABA immunoreactivity of 12.39 and 14.05 are omitted from the distribution for the sake of clarity.

we were unable to test for the presence of glutamate immunoreactivity in ChAT-positive structures in the EP.

Synaptic organization and functional considerations

It is now recognized that neurons of the direct and indirect pathways of information flow through the basal ganglia, which have functionally different roles in the control of movement, and provide different patterns of innervation of the output neurons of the basal ganglia. Thus input from the indirect pathways, i.e. from the globus pallidus and the subthalamic nucleus, occurs in the more proximal regions of the neurons whereas that from the direct pathway, i.e. from the neostriatum, occurs in both distal and proximal parts of the neurons. The anterogradely labelled terminals identified in the present study formed asymmetrical synaptic contacts with all parts of entopeduncular neurons that were examined. The findings of previous anterograde labelling studies (Bolam and Smith, 1992; Bolam *et al.*, 1993; Bevan *et al.*, 1994) and the neurochemical findings in the present study enabled us to identify striatal-like, pallidal-like and subthalamic-like boutons in the EP and thus examine the relationship between the anterogradely labelled terminals and the innervation by neurons of the direct and indirect pathways. Anterogradely labelled terminals from the MTg made synaptic contact with the same neurons in the EP that received input from terminals derived from the neostriatum and from both the globus pallidus and subthalamic nucleus. This synaptic convergence implies that the input from the MTg can directly modulate, or influence, the output of the basal ganglia by interacting with the major pathways of information flow through the basal ganglia. By convergence with striatal terminals, MTg terminals are in a position to modulate the direct pathway (i.e. cortex–neostriatum–EP) and by convergence with pallidal and subthalamic terminals they are in a position to modulate the indirect pathways.

This study demonstrates the anatomical and neurochemical substrates of the excitatory input of the MTg to entopeduncular neurons that have been previously reported electrophysiologically (Gonya-Magee and Anderson, 1983; Scarnati *et al.*, 1988). The presence of a glutamatergic component and possibly also a cholinergic component to this projection, and previous findings of glutamatergic and cholinergic inputs from the MTg to other structures, including the substantia nigra pars compacta in the squirrel monkey (Lavoie and Parent, 1994c), the dopaminergic neurons of the substantia nigra pars compacta in the rat (Futami *et al.*, 1995) and the subthalamic nucleus in the rat (Bevan and Bolam, 1995), demonstrate that the MTg has the potential to exert widespread effects at many levels of the basal ganglia. The projection from the MTg to the EP, as well as to other regions of the basal ganglia, thus represents an interface between the basal ganglia, which have important roles in movement, and brainstem systems involved in locomotion, sleep–wake cycles and arousal.

Acknowledgements

The authors thank Jason Hanley for his help in the initial stages of the work and Liz Norman, Caroline Francis, Paul Jays and Frank Kennedy for technical assistance. We also thank Peter Somogyi for the GABA antiserum and Veronique Bernard and Jason Hanley for comments on the manuscript. This work was funded by the Wellcome Trust and the Medical Research Council, UK. N. P. C. is in receipt of an MRC Research Studentship.

Abbreviations

BDA	biotinylated dextran amine
ChAT	choline acetyltransferase
EP	entopeduncular nucleus
GABA	γ-aminobutyric acid
LDTg	lateral dorsal tegmental region
MEA	midbrain extrapyramidal area
MTg	mesopontine tegmentum
NADPH	nicotinamide adenine dinucleotide phosphate
PB	0.1 M phosphate buffer, pH 7.4
PBS	phosphate-buffered saline
PHA-L	*Phaseolus vulgaris* leucoagglutinin
PPN-Ch5	area defined by the cholinergic neurons of the pedunculopontine region
TBS	Tris-buffered saline
TMB	tetramethylbenzidine
WGA-HRP	wheat germ agglutinin conjugated to horseradish peroxidase

References

Abdullah, L. H., Ordronneau, P. and Petrusz, P. (1992) Molecular requirements for hapten binding to antibodies against glutamate and aspartate. *Neuroscience*, **51**, 729–738.

Bevan, M. D. and Bolam, J. P. (1995) Cholinergic, GABAergic and glutamate-enriched inputs from the mesopontine tegmentum to the subthalamic nucleus in the rat. *J. Neurosci.*, **15**, 7105–7120.

Bevan, M. D., Crossman, A. R. and Bolam, J. P. (1994) Neurons projecting from the entopeduncular nucleus to the thalamus receive convergent synaptic inputs from the subthalamic nucleus and the neostriatum in the rat. *Brain Res.*, **659**, 99–109.

Bevan, M. D., Francis, C. M. and Bolam, J. P. (1995) The glutamate-enriched cortical and thalamic input to neurons in the subthalamic nucleus of the rat: convergence with GABA-positive terminals. *J. Comp. Neurol.*, **361**, 491–511.

Bolam, J. P. and Smith, Y. (1992) The striatum and the globus pallidus send convergent synaptic inputs onto single cells in the entopeduncular nucleus of the rat: a double anterograde labelling study combined with post-embedding immunocytochemistry for GABA. *J. Comp. Neurol.*, **321**, 456–476.

Bolam, J. P., Smith, Y., Ingham, C. A., von Krosigk, M. and Smith, A. D. (1993) Convergence of synaptic terminals from the striatum and the globus pallidus onto single neurones in the substantia nigra and the entopeduncular nucleus. *Prog. Brain Res.*, **99**, 73–88.

Butcher, L. L. and Semba, K. (1989) Reassessing the cholinergic basal forebrain: nomenclature, schemata and concepts. *Trends Neurosci.*, **12**, 483–485.

Charara, A. and Parent, A. (1994) Brainstem dopaminergic, cholinergic and serotoninergic afferents to the pallidum in the squirrel monkey. *Brain Res.*, **640**, 155–170.

Clarke, N. P., Hanley, J. J., Bevan, M. D. and Bolam, J. P. (1995) Origin, synaptology and neurochemistry of the projection from the mesopontine tegmentum to the entopeduncular nucleus and neostriatum in the rat. *Brain Res. Assoc. Abstr.*, **12**, 39.

Clements, J. R. and Grant, S. (1990) Glutamate-like immunoreactivity in neurons of the laterodorsal tegmental and pedunculopontine nuclei in the rat. *Neurosci. Lett.*, **120**, 70–73.

Clements, J. R., Toth, D. D., Highfield, D. A. and Grant, S. J. (1991) Glutamate-like immunoreactivity is present within cholinergic neurons of the laterodorsal tegmental and pedunculopontine nuclei. *Adv. Exp. Med. Biol.*, **295**, 127–142.

DeVito, J. L., Anderson, M. E. and Walsh, K. E. (1980) A horseradish peroxidase study of afferent connections of the globus pallidus in *Macaca mulatta*. *Exp. Brain Res.*, **38**, 65–73.

Ericson, A.-M., Blomqvist, A., Craig, A. D., Ottersen, O. P. and Broman, J. (1995) Evidence for glutamate as neurotransmitter in trigemino- and spinothalamic tract terminals in the nucleus submedius of cats. *Eur. J. Neurosci.*, **7**, 305–317.

Futami, T., Takakusaki, K. and Kitai, S. T. (1995) Glutamatergic and cholinergic inputs from the pedunculopontine tegmental nucleus to dopamine neurons in the substantia nigra pars compacta. *Neurosci. Res.*, **21**, 331–342.

Garcia-Rill, E. (1991) The pedunculopontine nucleus. *Prog. Neurobiol.*, **36**, 363–389.

Gerfen, C. R. and Sawchenko, P. E. (1984) An anterograde neuroanatomical tracing method that shows the detailed morphology of neurons, their axons and terminals: immunohistochemical localization of an axonally transported plant lectin *Phaseolus vulgaris*-leucoagglutinin (PHA-L). *Brain Res.*, **290**, 219–238.

Gonya-Magee, T. and Anderson, M. E. (1983) An electrophysiological characterization of projections from the pedunculopontine area to entopeduncular nucleus and globus pallidus in the cat. *Exp. Brain Res.*, **49**, 269–279.

Graybiel, A. M. (1977) Direct and indirect preoculomotor pathways of the brainstem: an autoradiographic study of the pontine reticular formation in the cat. *J. Comp. Neurol.*, **175**, 37–78.

Hepler, J. R., Toomim, C. S., McCarthy, K. D., Conti, F., Battaglia, G., Rustioni, A. and Petrusz, P. (1988) Characterization of antisera to glutamate and aspartate. *J. Histochem. Cytochem.*, **36**, 13–22.

Hodgson, A. J., Penke, B., Erdei, A., Chubb, I. W. and Somogyi, P. (1985) Antisera to γ-aminobutyric acid. I. Production and characterization using a new model system. *J. Histochem. Cytochem.*, **33**, 229–239.

Hopwood, D. (1972) Theoretical and practical aspects of glutaraldehyde fixation. *Histochem. J.*, **4**, 267–303.

Jackson, A. and Crossman, A. R. (1983) Nucleus tegmenti pedunculopontinus: efferent connections with special reference to the basal ganglia, studied in the rat by anterograde and retrograde transport of horseradish peroxidase. *Neuroscience*, **10**, 725–765.

Jones, B. E. (1990) Relationship of GABAergic to cholinergic neurons within the laterodorsal and pedunculopontine tegmental nuclei. *Soc. Neurosci. Abstr.*, **16**, 300.

Jones, B. E. (1993) The organization of central cholinergic systems and their functional importance in sleep–waking states. *Prog. Brain Res.*, **98**, 61–71.

Kharazia, V. N. and Weinberg, R. J. (1994) Glutamate in thalamic fibers terminating in layer IV of primary sensory cortex. *J. Neurosci.*, **14**, 6021–6032.

Lai, Y. Y., Clements, J. R. and Siegel, J. M. (1993) Glutamatergic and cholinergic projections to the pontine inhibitory area identified with horseradish peroxidase retrograde transport and immunohistochemistry. *J. Comp. Neurol.*, **336**, 321–330.

Lavoie, B. and Parent, A. (1994a) Pedunculopontine nucleus in the squirrel monkey: distribution of cholinergic and monoaminergic neurons in the mesopontine tegmentum with evidence for the presence of glutamate in cholinergic neurons. *J. Comp. Neurol.*, **344**, 190–209.

Lavoie, B. and Parent, A. (1994b) Pedunculopontine nucleus in the squirrel monkey: projections to the basal ganglia as revealed by anterograde tract-tracing methods. *J. Comp. Neurol.*, **344**, 210–231.

Lavoie, B. and Parent, A. (1994c) Pedunculopontine nucleus in the squirrel monkey: cholinergic and glutamatergic projections to the substantia nigra. *J. Comp. Neurol.*, **344**, 232–241.

Lee, H. J., Rye, D. B., Hallenger, A. E., Levey, A. I. and Wainer, B. H. (1988) Cholinergic vs noncholinergic efferents from the mesopontine tegmentum to the extrapyramidal motor system nuclei. *J. Comp. Neurol.*, **275**, 469–492.

Levey, A. I., Edmunds, S. M., Heilman, C. J., Desmond, T. J. and Frey, K. A. (1994) Localization of muscarinic m3 receptor protein and M3 receptor binding in rat brain. *Neuroscience*, **63**, 207–221.

Llewellyn-Smith, I. J., Phend, K. D., Minson, J. B., Pilowsky, P. M. and Chalmers, J. P. (1992) Glutamate-immunoreactive synapses on retrogradely-labelled sympathetic preganglionic neurons in rat thoracic spinal cord. *Brain Res.*, **581**, 67–80.

Mesulam, M., Mash, D., Hersh, L., Bothwell, M. and Geula, C. (1992) Cholinergic innervation of the human striatum, globus pallidus, subthalamic nucleus, substantia nigra and red nucleus. *J. Comp. Neurol.*, **323**, 252–268.

Nakanishi, H., Kita, H. and Kitai, S. T. (1991) Intracellular study of rat entopeduncular nucleus neurons in an *in vitro* slice preparation: response to subthalamic stimulation. *Brain Res.*, **549**, 285–291.

Ottersen, O. P. (1989) Quantitative electron microscopic immunocytochemistry of neuroactive amino acids. *Anat. Embryol.*, **180**, 1–15.

Ottersen, O. P. and Storm-Mathisen, J. (1989) Excitatory and inhibitory amino acids in the hippocampus. In Chan-Palay, V. and Kohler, C. (eds), *The Hippocampus: New Vistas*. Alan R. Liss, New York.

Paxinos, A. and Watson, C. (1986) *The Rat Brain in Stereotaxic Coordinates*. Academic Press, Sydney.

Petrusz, P., Van Eyck, S. L., Weinberg, R. J. and Rustioni, A. (1990) Antibodies to glutamate and aspartate recognize non-endogenous ligands for excitatory amino acid receptors. *Brain Res.*, **529**, 339–344.

Phend, K. D., Weinberg, R. J. and Rustioni, A. (1992) Techniques to optimize post-embedding single and double staining for amino acid neurotransmitters. *J. Histochem. Cytochem.*, **40**, 1011–1020.

Rinvik, E. and Ottersen, O. P. (1993) Terminals of subthalamonigral fibres are enriched with glutamate-like immunoreactivity: an electron microscopic, immunogold analysis in the cat. *J. Chem. Neuroanat.*, **6**, 19–30.

Rye, D. B., Saper, C. B., Lee, H. J. and Wainer, B. H. (1987) Pedunculopontine tegmental nucleus of the rat: cytoarchitecture, cytochemistry, and some extrapyramidal connections of the mesopontine tegmentum. *J. Comp. Neurol.*, **259**, 483–528.

Saper, C. B. and Loewy, A. D. (1982) Projections of the pedunculopontine tegmental nucleus in the rat: evidence for additional extrapyramidal circuitry. *Brain Res.*, **252**, 367–372.

Scarnati, E., Di Loreto, S., Proia, A. and Gallie, G. (1988) The functional role of the pedunculopontine nucleus in the regulation of the electrical activity of entopeduncular neurons in the rat. *Arch. Ital. Biol.*, **126**, 145–163.

Smith, Y. and Parent, A. (1988) Neurons of the subthalamic nucleus in primates display glutamate but not GABA immunoreactivity. *Brain Res.*, **453**, 353–356.

Somogyi, P. and Hodgson, A. J. (1985) Antisera to γ-aminobutyric acid. III. Demonstration of GABA in Golgi-impregnated neurons and in conventional electron microscopic sections of cat striate cortex. *J. Histochem. Cytochem.*, **33**, 249–257.

Somogyi, P., Hodgson, A. J., Chubb, I. W., Penke, B. and Erdei, A. (1985) Antisera to γ-aminobutyric acid. II. Immunocytochemical application to the central nervous system. *J. Histochem. Cytochem.*, **33**, 240–248.

Somogyi, P., Halasy, K., Somogyi, J., Storm-Mathisen, J. and Ottersen, O. P. (1986) Quantification of immunogold labelling reveals enrichment of glutamate in mossy and parallel fibre terminals in cat cerebellum. *Neuroscience*, **19**, 1045–1050.

Spann, B. M. and Grofova, I. (1989) Origin of ascending and spinal pathways from the nucleus tegmenti pedunculopontinus in the rat. *J. Comp. Neurol.*, **283**, 13–27.

Spann, B. M. and Grofova, I. (1992) Cholinergic and non-cholinergic neurons in the pedunculopontine tegmental nucleus. *Anat. Embryol.*, **186**, 215–227.

Steininger, T. L., Rye, D. B. and Wainer, B. H. (1992) Afferent projections to the cholinergic pedunculopontine tegmental nucleus and adjacent midbrain extrapyramidal area in the albino rat. I. Retrograde tracing studies. *J. Comp. Neurol.*, **321**, 515–543.

Valtschanoff, J. G., Phend, K. D., Bernardi, P. S., Weinberg, R. J. and Rustioni, A. (1994) Amino acid immunocytochemistry of primary afferent terminals in the rat dorsal horn. *J. Comp. Neurol.*, **346**, 237–252.

Van den Pol, A. N. (1991) Glutamate and aspartate immunoreactivity in hypothalamic presynaptic axons. *J. Neurosci.*, **11**, 2087–2101.

Veenman, C. L., Reiner, A. and Honig, M. G. (1992) Biotinylated dextran amine as an anterograde tracer for single-labelling and double-labelling studies. *J. Neurosci. Methods*, **41**, 239–254.

Vincent, S. R., Satoh, K., Armstrong, D. M. and Fibiger, H. C. (1983) NADPH-diaphorase: a selective histochemical marker for the cholinergic neurons of the pontine reticular formation. *Neurosci. Lett.*, **43**, 31–36.

Von Krosigk, M. and Smith, A. D. (1991) Descending projection from the substantia nigra and retrorubral field to the medullary and pontomedullary reticular formation. *Eur. J. Neurosci.*, **3**, 260–273.

Wainer, B. H., Levey, A. I., Mufson, E. J. and Mesulam, M.-M (1984) Cholinergic systems in mammalian brain identified with antibodies against choline acetyltransferase. *Neurochem. Int.*, **6**, 163–182.

Weinberg, R. J. and Van Eyck, S. L. (1991) A tetramethylbenzidine/tungstate reaction for horseradish peroxidase histochemistry. *J. Histochem. Cytochem.*, **39**, 1143–1148.

Woolf, N. J. (1991) Cholinergic systems in mammalian brain and spinal cord. *Prog. Neurobiol.*, **37**, 475–524.

Woolf, N. J. and Butcher L. L. (1986) Cholinergic systems in the rat brain: III. Projections from the pontomesencephalic tegmentum to the thalamus, tectum, basal ganglia and basal forebrain. *Brain Res. Bull.*, **16**, 603–637.